European Review for Medical and Pharmacological Sciences 2017; 21: 4952-4965

Resveratrol transcriptionally regulates miRNA-18a-5p expression ameliorating diabetic nephropathy via increasing autophagy

X.-H. XU[1,2], D.-F. DING[2], H.-J YONG[2], C.-L DONG[3], N. YOU[2], X.-L. YE[2], M.-L. PAN[2], J.-H. MA[1], Q. YOU[4], Y.-B. LU[2]

[1]Department of Endocrinology, Nanjing First Hospital Affiliated to Nanjing Medical University, Nanjing, Jiangsu, China
[2]Department of Endocrinology, The Second Affiliated Hospital of Nanjing Medical University, Nanjing, Jiangsu, China
[3]Department of Emergency, Yancheng First People's Hospital, Yancheng, China
[4]Department of Geriatics, The Second Affiliated Hospital of Nanjing Medical University, Nanjing Medical University, Nanjing, China

Xianghong Xu and Dafa Ding contributed equally to this study

Abstract. – OBJECTIVE: To investigate the effects of resveratrol on autophagy in the chronically diabetic nephropathy and to study the effects of the different expression of microRNAs after resveratrol (RSV) treated in db/db mice (diabetic mice).

MATERIALS AND METHODS: Db/m (non- diabetic) and db/db mice were randomly divided into to intra gastric RSV treatment group or control group. Renal tissues were prepared for HE/PAS staining. In vitro, mouse podocytes cell lines were grown in different mediums with different dose of resveratrol treatment. microRNA (miRNA) gene chips assay was performed for differentially expressed miRNAs screening. Western blot was used to detect protein levels.

RESULTS: *In vivo*, RSV significantly decreased urinary albumin, serum creatinine, mesangial area and glomerular size in db/db mice. After RSV treatment, LC3-II/LC3-I and synaptopodin were increased while cleaved-caspase 3 was decreased in kidney tissues. In vitro, podocytes treated with RSV exhibited significantly increased LC3-II/LC3-I and decreased cleaved caspase 3. Moreover, this effect of RSV can be enhanced by rapamycin (RAPA, an activator of autophagy) but partially reversed by 3-MA (an autophagy inhibitor). Further, we found that miR-18a-5p was significantly upregulated after RSV treatment in db/db mice. Overexpression of miR-18a-5p in podocytes resulted in significant inhibition of cleaved-caspase 3 protein, and increased the ratio of LC3-II/LC3-I. Dual luciferase report assay validated that Atactic telangiectasis mutation (ATM) was a target of miR-18a-5p. In podocytes, downregulation of cleaved caspase 3 and the enhanced ratio of protein LC3-II/LC3-I were detected in cells transfected with ATM siRNA.

CONCLUSIONS: Role of miRNA-18a-5p in the regulation of autophagy via targeting ATM may represent a promising therapeutic target for preventing and attenuating diabetic nephropathy.

Key Words:
Resveratrol, Diabetic nephropathy, Podocyte, Autophagy, microRNA.

Introduction

Diabetic nephropathy is the most common cause of end-stage kidney disease worldwide. The increasing prevalence of diabetic nephropathy results in considerable mortality and morbidity. Podocytes are a major component of the glomerular filtration barrier. Injury and loss of podocytes lead to albuminuria, a hallmark of diabetic nephropathy and a predictor for the progression of kidney diseases. So, there is an urgent need to identify new therapeutic target molecules underlying the pathogenesis of diabetic nephropathy, in order to establish alternative therapeutic options.

Autophagy, a term which was first coined by Christian de Duve in 1963, is derived from the Greek and meaning "self-eating". Autophagy is a eukaryotic, evolutionarily conserved catabolic process in which unnecessary or dysfunctional cellular components are sequestered in double-membrane vesicles and delivered to the lysosomal machinery for degradation. Autopha-

Corresponding Author: Yibing Lu, MD; e-mail: luyibing2004@126.com

gy, a multi-step lysosomal degradation process with function to degrade long-lived proteins and damaged organelles, maintains intracellular homeostasis and cell integrity[1]. Studies indicate that diabetic kidneys are deficient in autophagy activity[2]. Several studies suggest that finding the key target in activating and restoring autophagy activity might be renoprotective in the disease[3-6].

Podocytes, derived from embryonic precursor mesenchymal cells, are considered terminally differentiated cells in the mature kidney[7,8]. As highly differentiated neuron-like epithelial cells, podocytes have a very limited capacity for cell division and replenishment[9]. Evidence shows that podocytes have a high level of basal autophagy, which may serve as a mechanism for their maintenance of cellular homeostasis[10]. The ability to maintain homeostasis under certain pathophysiological stress seems to be very important in determining the fate of podocytes.

3,5,4′ trihydroxystilbene, or resveratrol (RSV), a natural polyphenolic compound found in grapes and red wine, is reported to have beneficial effects on renal diseases[11-13]. Many studies show that RSV exerts its protective effects through antioxidant activity and silent mating type information regulation 2 homolog-*1 (*SIRT1) activation[13-16]. Some of the benefits of RSV are mediated by stimulation of autophagy. RSV is an autophagy promoter in some cases and protects from oxidative damage and inflammation[17-19]. However, there is little information on the molecular mechanism of RSV ameliorating nephropathy in type 2 diabetes through regulating autophagy.

MicroRNAs (miRNAs) are endogenous ~23 nucleotides (nt) RNAs, regulating gene expression by pairing to the mRNAs of protein-coding genes to direct their post-transcriptional repression[20]. Numerous miRNAs regulate programmed cell death including apoptosis, autophagy and necroptosis[21]. Establishing miRNA expression changes that occur during pathologic conditions allows the identification of potential biomarkers and therapeutic targets. Here, we first investigated the effects of resveratrol on the progression of diabetic nephropathy and the apoptosis of renal cortex in db/db mice and cultured human podocytes. Then, we explored whether resveratrol improved the level of autophagy in the db/db mice's renal cortex and cultured podocytes.

Furthermore, we identified miRNAs differentially expressed in normal and db/db mice and db/db mice treated with RSV by microarray analysis of mouse kidney cortex samples. Finally, we explored whether resveratrol regulates autophagy and apoptosis in db/db mice and human podocytes through the regulation of miRNA.

Materials and Methods

Animal Model

All of the following details of the study were approved by Institutional Review Board of Nanjing Medical University.

Eight week-old male db/db mice and lean wild type db/m mice were purchased from the Model Animal Research Center of Nanjing University (Nanjing, China). Animals were housed at constant room temperature (20±1°C) under a controlled 12 h light to 12 h dark cycle and had free access to water and food. Animal studies were approved by the Nanjing Medical University of Chinese Medicine Institutional Animal Care and Use Committee.

The experimental mice were randomly allocated to the following groups (n=8-10 per group): Group 1: wild type mice fed regular chow (db/m group), Group 2: wild type mice fed regular chow and given with RSV by gavage (db/m + RSV group), Group 3: db/db mice fed regular chow (db/db group), and Group 4: db/db mice fed regular chow and given with RSV by gavage (db/db + RSV group). The db/m + RSV group and db/db + RSV group were given with RSV at a dose of 100 mg/Kg once a day for 12 weeks by intragastric administration. The db/m group and db/db group were given with 0.5% carboxymethyl cellulose sodium (CMC) at a dose of 100 ml/kg once a day for 12 weeks by intragastric administration. RSV was purchased from Sigma-Aldrich (St. Louis, MO, USA), and in 0.5% CMC. The concentration of RSV is 1 g/mL.

Tail blood glucose (TBG) levels were monitored consecutively. Experiment and blood glucose levels of all groups were measured using glucose test reagent strips (Accu-Check Active Glucose test strips, Roche, Mannheim, Germany) with a glucometer (Accu-Check Active, Roche, Mannheim, Germany) in samples obtained from the tail vein. All mice from each group were housed in metabolic cages in order to collect 24 h urine samples at 12-week after the treatment. Then, mice were sacrificed. Serum was collected and the kidneys were removed. A kidney was immediately frozen in liquid nitrogen and stored at -80°C for RNA and protein analysis and the other was dropped in 4% paraformaldehyde for histopathological analysis.

Urinary Albumin and Serum Creatinine Assay

Urinary albumin was measured by using a mouse Albumin ELISA Quantitation Kit according to the manufacturer's protocol (Bethyl Laboratories, Mouse Albumin ELISA Kit, E99-134, Montgomery, TX, USA). Serum creatinine was measured by using a Serum Creatinine Detection Kit according to the manufacturer's protocol (Arbor Assays, Detect X Serum creatinine Kit, KB02-H2, Ann Arbor, MI, USA).

Glomerular Morphological Analysis

Renal tissues were embedded in paraffin, and 4-μm-thick sections were prepared for *he*matoxylin-eosin (HE) staining and periodic acid schiff (PAS) staining. The sections of renal glomeruli from mice of each group were observed under microscope. The average diameter of glomeruli was measured with image analysis software (Image-pro plus, Version 5.1.0.20, Media Cybernetics, Inc., Rockville, MD, USA). Glomerular tufts in a group were counted in nine different visual fields.

Double Immunofluorescence Labeling

Double immunofluorescence labeling experiments were used to analyze the synaptopodin expression and to demonstrate the changes of autophagosomes. Snap-frozen sections (3 μm), were fixed in cold acetone, blocked in 3% bovine serum albumin (BSA) and then incubated with primary goat polyclonal antibody against LC3B (Santa Cruz, CA, USA) after washing secondary fluorescein isothiocyanate (FITC)-conjugated anti-goat IgG antibody (Abbkine, Wuhan, China). The process was repeated for the rabbit polyclonal anti-synaptopodin (Abcam, Cambridge, MA, USA). Then, secondary goat anti-rabbit DyLight 594 antibodies (Abbkine, Wuhan, China) were added for 1 h at room temperature. After counterstaining with DAPI to visualize the nuclei, photographs were obtained using a fluorescent microscope (Olympus, Tokyo, Japan). On average, 20 randomly selected hilar glomerular tuft cross-sections were assessed per mouse. In each experimental setting, immunofluorescence images were captured with identical light exposure times. Slides were measured with image analysis software (Image-pro plus, Version 5.1.0.20, Media Cybernetics, Inc., Rockwille, MD, USA). Results were calculated as percentage positively stained tissue within the glomerular tuft. On average, 20 randomly selected hilar glomerular tuft cross-sections were assessed per mouse.

miRNA Screening and Target Prediction

Total RNAs were quantified by the NanoDrop ND-2100 (Thermo Scientific, Waltham, MA, USA) and the RNA integrity was assessed using Agilent 2100 (Agilent Technologies, Santa Clara, CA, USA). The sample labeling, microarray hybridization, and washing were performed based on the manufacturer's standard protocols. Briefly, total RNA were tailed with Poly A and labeled with Biotin. The labeled RNAs were hybridized onto the microarray. After being washed, the arrays were scanned by the Affymetrix Scanner 3000 (Affymetrix, Santa Clara, CA, USA). Affymetrix Gene Chip Command Console software (version 4.0, Affymetrix, Santa Clara, CA, USA) was used to analyze array images to get raw data. Next, Genespring software (Version 12.5; Agilent Technologies, Santa Clara, CA, USA) was used to proceed the following data analysis. Differentially expressed miRNAs were identified through fold changes. The threshold set for up- and down-regulated genes was a fold change ≥ 2.0. Target genes of differentially expressed miRNAs were the intersection predicted with 3 databases (Targetscan, PITA, microRNA.org).

Luciferase Reporter Gene Assay

Using Targetscan software, ATM was predicted to be a target of miR-18a-5p. The construct of ATM 3'UTR was generated by Shenzhen Huaanpingkang Company (Shenzhen, China). The full length 3'-UTR of ATM was amplified by PCR from mice genomic DNA and cloned at the BamHI and XhoI sites into luciferase reporter vector (Promega, Madison, WI, USA). 293 T cells were co-transfected with a reporter construct of m-Atm-3'UTR and miR-18a-5p mimic or miR-negative control. After 48 h of incubation, the luciferase activities were measured in a luminometer with the Dual-Luciferase Reporter Assay System (Promega, Madison, WI, USA) according to the manufacturer's recommendations.

Culture of Podocytes

The conditionally immortalized mouse podocyte cell line was kindly provided by Dr. Junwei Yang (Department of Endocrinology, Second Affiliated Hospital of Nanjing Medical University, Nanjing, China) while their cell lines were provided by Dr Peter Mundel (Mount Sinai School of Medicine, New York, NY, USA) and described previously[22]. Cells were grown on dishes coated with type I collagen (Sigma-Aldrich, Inc., St. Louis, MO, USA) and were cultured

at the permissive temperature (33°C) in Roswell Park Memorial Institute 1640 (RPMI-1640) medium supplemented with 10% fetal bovine serum (FBS) Invitrogen (Carlsbad, CA, USA), 100 U/mL penicillin, and 100 U/mL streptomycin, and recombinant interferon-γ (Invitrogen, Carlsbad, CA, USA). To induce differentiation, podocytes were grown under non-permissive conditions at 37°C for 10 to 14 days in the absence of interferon-γ. After serum starvation for 16 h, cells exposed to the treatment for the indicated time periods.

Treatments and Study Design

First, podocytes were grouped into five: Control (Grow in normal medium with 5 mmol/L glucose), Glu (Grow in medium with 30 mmol/L glucose for 12 hours), Glu+RSV 1 μM (Grow in medium with 30 mmol/L glucose and 1 Mm RSV for 12 h), Glu+RSV 10 μM (Grow in medium with 30 mmol/L glucose and 10 μmol/L RSV for 12 h), Glu+RSV 100 μM (Grow in medium with 30 mmol/L glucose and 100 μmol/L RSV for 12 h). Second, podocytes were divided into five groups: Control (Grow in normal medium with 5 mmol/L glucose), Glu (Grow in medium with 30 mmol/L glucose for 12 h), Glu+RSV (Grow in medium with 30 mmol/L glucose and 10 μmol/L RSV for 12 h), Glu+RSV+ 3-methyladenine (3-MA) (Grow in medium with 30 mmol/L glucose, 10 μmol/L RSV and 5 mmol/L3-MAfor 12 h), Glu+RSV+RAPA (Grow in medium with 30 mmol/L glucose, 10 μmol/L RSV and 100 nmol/L rapamycin for 12 h). As an osmotic control, podocytes were cultured in medium containing 5 mmol/L normal glucose plus 25 mmol/L mannitol. RSV, 3-MA and rapamycin were diluted in dimethylsulfoxide (DMSO), so the control groups received an equal volume of dimethyl sulfoxide (DMSO).

Mimic and Inhibitor miRNA Transfection

Podocytes were planted into 6-well plates, at 50% confluence when transfection was performed. All of the transient transfections were performed with Lipofectamine 2000 Reagent (Invitrogen, Carlsbad, CA, USA) according to the manufacturer's recommendations. Then, 5 μL 20 μM miR-18a-5p mimic or mimic negative control miRNA or miR18a-5p-inhibitor or inhibitor negative control (Genepharma, Shanghai, China) diluted with 250 μL Opti-MEM and 5 μL Lipofectamine 2000 diluted with 250 mL Opti-MEM were mixed together, and kept at room temperature for 20 min, dropped into 20 mm plate with total 500 μL medium. After 6 h of transfection, the medium was replaced with RPMI-1640. After 6 h, cells were incubated for 48 h with fresh medium. At last, protein or RNA was harvested. Transfection efficiency (> 90%) was measured by qRT-PCR.

SiRNA Transfection

Podocytes were planted into 6-well plates in 2 mL antibiotic-free normal growth medium supplemented with FBS, at 60% confluence when transfection was performed. SiRNA transfection medium and siRNA transfection reagent were purchased from Santa Cruz Biotechnology (Santa Cruz, CA, USA). Solution A: 6 μl of siRNA duplex was diluted into 100 μL siRNA transfection medium. Solution B: 6 μl of siRNA transfection reagent was diluted into 100 μL siRNA transfection medium. siRNA duplex solution was added (Solution A) directly to the dilute transfection reagent (Solution B) using a pipette, and it was mixed gently by pipetting the solution up and down. Then, the mixture was incubated 15-45 min at room temperature. The cells were washed once with 2 mL of siRNA transfection medium. The medium was aspirated and we proceed immediately to the next step. 0.8 mL siRNA transfection medium was added to each tube containing the siRNA transfection reagent mixture (Solution A + Solution B). The mixture was mixed gently and overlaid onto the washed cells. The cells were incubated 6 h at 37°C in a CO_2 incubator. Fluorescein conjugated control siRNA should only be incubated for a total of 6 h at 37°C in a CO_2 incubator. At the end of incubation, they are ready to be assayed by fluorescent microscopy. Without removing the transfection mixture, 1 mL of normal growth medium containing antibiotics was added. Then, the cells were incubated for additional 18 h in fresh medium.

Real-time Quantitative PCR (qRT-PCR)

For the experiments using mouse kidney tissue and the cell culture experiments, total RNA, including microRNA, was extracted using TRIzol reagent (Invitrogen, Carlsbad, CA, USA) and miRNA easy mini kit (Qiagen, Hilden, Germany) according to the manufacturer's instructions. A sample of total RNA (2 μg) was reverse transcribed with 200 U Moloney murine leukemia virus reverse transcriptase (Promega, Madison, WI, USA) in the presence of 0.5 mM deoxynucleotide triphosphate, 25 U ribonuclease inhibitor, and 10 mM random hexamer primers,

Table I. Effect of resveratrol on glucose, creatinine and albuminuria (db/m group, db/m + RSV group, db/db group and db/db + RSV group).

	db/m	db/m + RSV	db/db	db/db + RSV
Glucose (mmol/L)	6.3±0.6	6.9±1.3	25.5±3.3*	24.2±3.9*
Creatinine (μmol/L)	29.85±6.94	31.54±7.32	50.13±8.15*	42.63±5.69*#
Urinary albumin (mg/24 h)	2.9±1.3	2.7±1.6	27.6±1.8*	16.4±1.8*#

Note: Data are shown as means ± SD (SD=Standard Deviation of 8 different mice), except for Urinary albumin where geometric mean tolerance factor. *significant difference versus db/m group at $p<0.05$. #significant difference vs. db/db group at $p<0.05$.

in a total volume of 25 μL. PCR primers were designed by Primer 5 software. Each quantitative Real-time PCR was carried out in a 25 μL volume of SYBR green Real-time PCR master mix (Roche, Mannheim, Germany) and analyzed using miScript II RT and SYBR green PCR kits. Individual samples were run in triplicate, and each experiment was repeated at least 3 times. The PCR cycling conditions were as follows: 10 min at 95°C, followed by 40 cycles of 15 s at 95°C and 60 s at 60°C. The temperature was heated from 60°C to 95°C, and the PCR melting curve was made every 1.0°C after the amplification reaction (ABI 7000; StepOnePlus, Danvers, MA, USA). The mRNA level of glyceraldehyde 3-phosphate dehydrogenase was used as an internal reference. For miRNA quantitative RT-PCR (qRT-PCR), a miRNA-specific stem-loop RT primer was hybridized to the miRNA and then reverse transcribed. Next, the reverse-transcribed product was amplified and monitored in quantitative Real-time PCR using a miRNA-specific upstream primer and the universal downstream primer (Supplemental Table II, universal downstream primer: 5'-GTGCAGGGTCCGAGGT-3'). U6 snRNA was used as an endogenous normalization control. Data analyses were performed using the comparative CT (ΔΔCT) method for calculating relative gene expression. mmu-U6 snRNA RT primer: RT primer:5'-GTCGTATCCAGTGCAGGGTCCGAGGTATTCGCACTGGATACGACAAAATA-3'; mmu -U6 snRNA primer (60 bp): Forward primer: 5'-GCGCGTCGTGAAGCGTTC -3'; Reverse primer: 5'-GTGCAGGGTCCGAGGT-3'; mmu-miR-18a-5p MIMAT0000072: 5'-UAAGGUGCAUCUAGUGCAGAUAG-3'; DNA: 5'-TAAGGTGCATCTAGTGCAGATAG-3'; 5'-ATTCCACGTAGATCACGTCTATC-3'; Forward: 5'-ACACTCCAGCTGGGTAAGGTGCATCTAGTGC-3'; Reverse: 5'-CTCAACTGGTGTCGTGGAGTCGGCAATTCAGTTGAGCTATCTGC-3' (72 bp).

Western Blot Analysis

Kidney tissues were homogenized by a polytron homogenizer (Brinkmann Instruments, Westbury, NY, USA) in radioimmunoprecipitation assay (RIPA) lysis buffer (1% NP-40, 0.1% SDS, 100 ug/mL phenylmethylsulfonyl fluoride (PMSF), 0.5% sodium deoxycholate, 1 mmol/L sodium orthovanadate, 2 μg/mL aprotinin, 2 ug/mL antipain, and 2 ug/mL leupeptin in PBS) on ice. The supernatants were collected after centrifugation at 16,000 *g* at 4°C for 30 min. Protein concentration was determined using a bicinchoninic acid (BCA) protein assay kit (Sigma-Aldrich, St.

Table II. Summary of expression levels' fold change of selected miRNAs.

	Fold Change	
miRNA name	[db/db] vs. [db/m]	[db/db+RSV] vs. [db/db]
mmu-miR-127-3p	3.3461757	-3.4468632
mmu-miR-133a-3p	4.803447	-2.5232022
mmu-miR-134-5p	3.0409434	-2.55692
mmu-miR-184-3p	2.009477	-2.995413
mmu-miR-205-5p	202.62115	-6.38806
mmu-miR-206-3p	5.579149	-4.6894283
mmu-miR-296-3p	2.3481312	-2.0693865
mmu-miR-31-5p	6.5910077	-4.768635
mmu-miR-329-3p	2.2464159	-2.2464159
mmu-miR-210-3p	2.844841	-2.2226272
mmu-miR-379-5p	2.3239453	-2.8354013
mmu-miR-382-5p	4.4397674	-4.081589
mmu-miR-541-5p	11.919057	-6.26631
mmu-miR-188-5p	-3.7823026	4.0109696
mmu-miR-18a-5p	-4.885903	2.789387
mmu-miR-714	-2.2514498	2.2514498
mmu-miR-7679-3p	-3.432294	2.718163

Note: MicroRNAs were either down-regulated in db/db+RSV vs. db/db group and meanwhile up-regulated in db/db vs. db/m group, or up-regulated in db/db+RSV vs. db/db group and meanwhile down-regulated in db/db vs. db/m group.

Table III. RT-PCR of miR-18a-5p confirmed miR-18a-5p-mimic resulted in miR-18a-5p overexpression and miR-18a-5p-inhibitor resulted in miR-18a-5p inhibition.

Group	miR-18a-5p(2-ΔΔCT Mean±Ct SI)
Control	1.001±0.048
mimic-NC	0.978±0.007
miR18a-5p-mimic	1.829±0.047
inhibitor NC	1.015±0.047
miR18a-5p-inhibitor	0.553±0.024
PS	0.018

Note: Podocytes were transfected with miR-18a-5p of inhibitors, mimics, NC, and Mock groups. Relative quantification relates the PCR signal of the target transcript in treatment groups to that an untreated control. The 2(-Delta Delta C(T)) method is used to analyze the relative changes in gene expression from Real-time quantitative PCR experiments. The data were represented as mean ± SD. $^{*}p<0.05$ was considered significant vs. control.

Louis, MO, USA), and whole tissue lysates were mixed with an equal amount of 2×SDS loading buffer (125 mmol/L Tris-HCl, 4% sodium dodecyl sulphate (SDS), 20% glycerol, 100 mmol/L DTT, and 0.2% bromophenol blue). Samples were heated at 100°C for 5-10 min before loading. Cells were grouped as above. Cells were lysed with RIPA buffer for 20 min on ice. Cells were harvested by scraping, centrifuged at 14,000 rpm for 15 min, and the supernatant was used for detection in Western blot analysis. Samples were separated on precast 10 or 12% SDS polyacrylamide gels (Bio-Rad, Hercules, CA, USA) and transferred onto nitrocellulose membranes. 30 mg of proteins were electrically transferred to polyvinylidene fluoride (PVDF) filters and incubated with anti-LC3 (SAB), anti-cleaved caspase-3(SAB), anti-synaptopodin (Abcam, Cambridge, MA, USA), anti-β-actin (SAB) or anti-GAPDH (SAB). Secondary antibodies corresponded to the respective primary antibodies. Chemiluminescence assay was performed with an electrochemiluminescence (ECL) Western blotting detection reagent according to manufacturer's instructions. Each membrane was stripped and probed for β-actin or GAPDH to verify equal protein loading.

Statistical Analysis

Western blotting, RT-PCR, and immunofluorescence staining were all repeated at least three times independently. For the histologic analysis and immunostaining, quantification was performed by using Image-Pro Plus 6.0 software (Version X; Media Cybernetics, Silver Springs, MD, USA). For Western blot analysis, quantitation was performed by scanning and analyzing the intensity of the hybridization signals using NIH imagine software. Statistical analysis was performed using Sigma Stat software (Jandel Scientific Software, San Rafael, CA, USA). Comparisons between groups were made using one-way ANOVA, followed by Student's *t*-test. $p<0.05$ was considered significant.

Results

In vivo, RSV Reduced Urinary Albumin in Diabetic db/db Mice

*Db/m*or *db/db* mice were treated with or without resveratrol for 12 weeks. Random blood glucose level, serum creatinine and 24 h urinary albumin were measured after 12 weeks of treatment with or without resveratrol. The diabetic mice (db/db group and db/db + RSV group) demonstrated a significant ($p<0.05$) escalation on the levels of blood glucose and urinary albumin when compared with control mice (db/m group) (Table I). The levels of urinary albumin and serum creatinine were significant ($p<0.05$) decreased when db/db mice were treated orally with RSV. Resveratrol treatment ameliorated albuminuria and decreased serum creatinine in a mouse model of type 2 diabetes.

Resveratrol Treatment Significantly Attenuates Renal Glomerular Injury in Diabetic Mice

To determine the therapeutic effect of resveratrol on diabetic renal lesion, mesangial matrix expansion and glomerular size were assessed by histochemistry. The results of HE/PAS staining showed that there was more extensive mesangial matrix expansion in the glomerulus in *db/db* mice than that in *db/m* mice, whereas resveratrol treatment significantly decreased the mesangial area in *db/db* mice. The glomerular size in *db/db* mice was larger than that in *db/m* mice, whereas resveratrol treatment significantly decreased glomerular size in *db/db* mice (Figure 1).

Autophagy is Further Induced and Apoptosis Reduced After RSV Treated in db/db Mice's Kidney

The above data showed that resveratrol could reduce urinary albumin in diabetic *db/db* mice. The autophagy was expected to involve in the effect of resveratrol on mice, thus the expression levels of proteins (LC3-II/LC3-I) involved

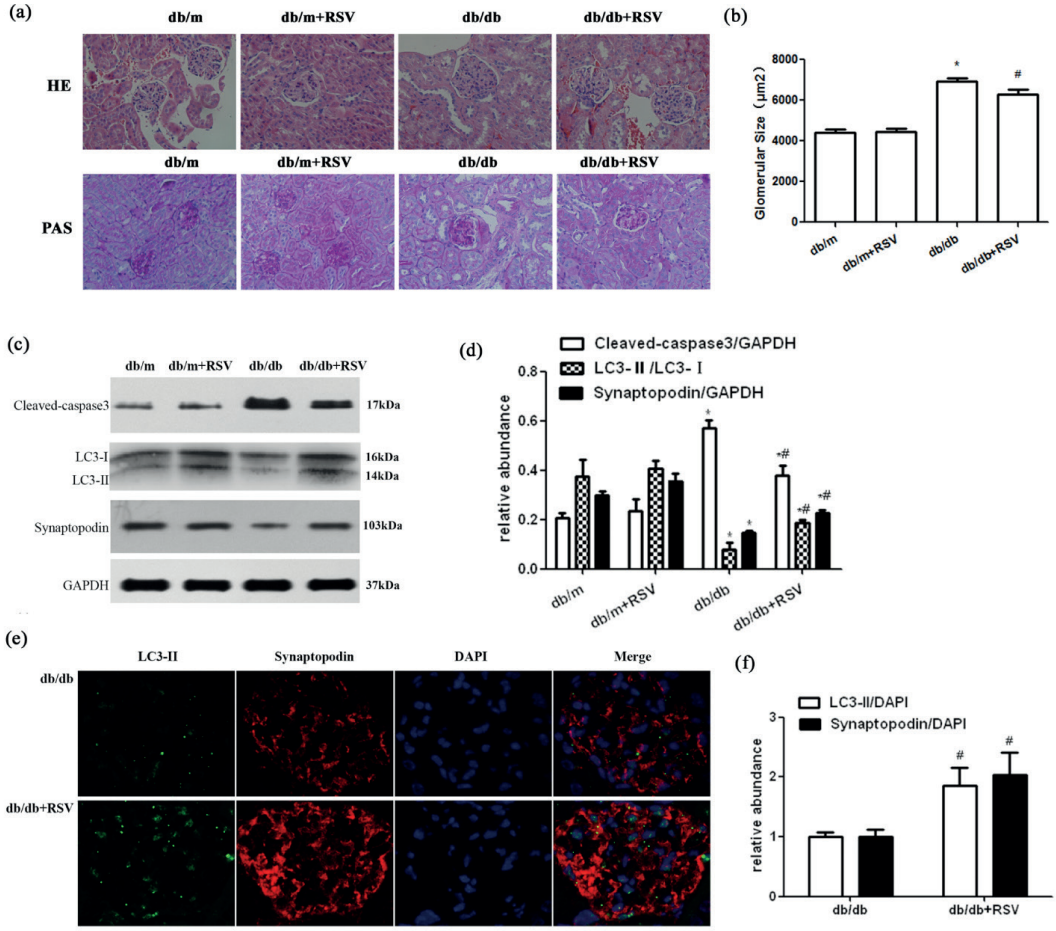

Figure 1. RSV treatment promoted autophagy in db/db mice. ***A*** and ***B:*** HE-staining and PAS-staining results in kidney sections; ***C*** and ***D***: resveratrol significantly increased LC3-II/LC3-I and synaptopodin, but decreased cleaved-caspase 3; E and ***F,*** Immunofluorescence staining of LC3-II and synaptopodin.

in autophagy were determined by Western blots analysis. The levels of cleaved-caspase 3 protein in kidney of db/db mice were higher than db/m mice, while resveratrol significantly decreased cleaved-caspase 3 expressions in mouse kidney (Figure 1c-d). On the contrary, the levels of LC3-II/LC3-I protein in kidney of db/db mice were lower than db/m mice, while resveratrol significantly increased the expressions of LC3-II/LC3-I protein in mouse kidney (Figure 1).

Protection of Resveratrol in Diabetic Kidney Might be via Protection of Podocytes

The above data showed resveratrol could protect diabetic kidney by inducing autophagy. So we investigated the distribution of autophagosomes in renal tissue by staining with LC3-II antibody, and the expression of synaptopodin by staining with anti-synaptopodin antibody in the two group mice (db/db group and db/db + RSV group). The double Immunofluorescence staining with LC3-II and synaptopodin shows there were much more LC3-II-positive cells and much more synaptopodin expression in resveratrol-treated diabetic mice than in resveratrol-untreated diabetic mice. These findings suggested a correlation between inducing autophagy and podocyte protection under diabetic conditions treated by resveratrol (Figure 1).

RSV Increased Autophagy and Suppressed Apoptosis in Podocytes Incubated in Medium Containing high Glucose

To examine the effect of RSV on HG-induced apoptosis and autophagy, podocytes were incubated in medium containing either high glucose (30 mmol/L), or high glucose plus RSV at three different concentration (1 μM, 10 μM, 100 μM).

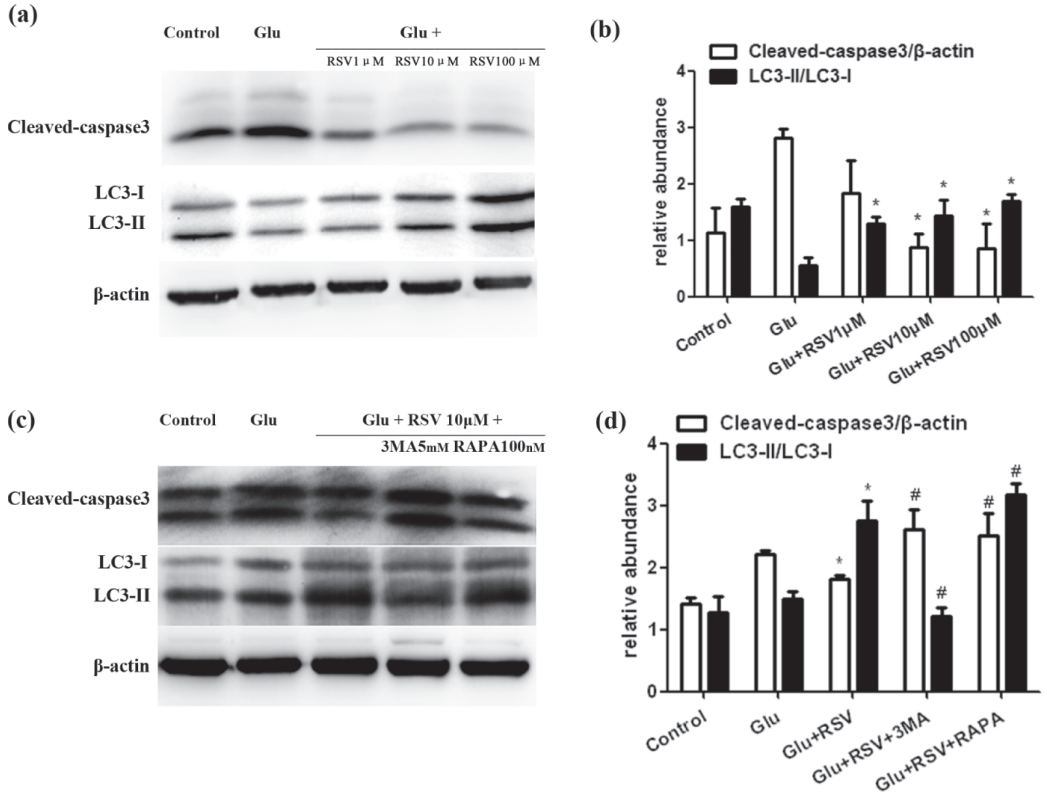

Figure 2. Effects of different concentration RSV on autophagy and apoptosis in podocytes. ***A*** and ***B***, LC3-II/LC3-I and cleaved caspase-3 in podocytes after pretreated with different concentrations of RSV of (0, 0.1, 10 and 100 **μmol**/L); C and D: LC3-II/LC3-I and cleaved caspase-3 in podocytes treated with 3MA or RAPA (Data are shown as means ± SD. *: significant difference *vs.* Glu Group at $p<0.05$).

First, we detected the autophagosome formation-related protein (the LC3 conversion) and the well-known marker for apoptosis (cleaved-caspas 3 protein). Compared with the group (HG treated cells), when co-treated with 10 μM RSV or 100 μM RSV, cells significantly increased the protein LC3-II/LC3-I ratio, while significantly decreased the protein expression of cleaved-caspase 3 (Figure 2a-b). So we think appropriate concentration (10 μM) of RSV decreases apoptosis *via* increasing autophagy. To further confirm the role of the autophagy, we used rapamycin (RAPA, which is regarded as an mTOR inhibitor and an activator of autophagy), and 3-Methyladenine (3-MA), a phosphatidylinositol 3-kinases (PI3K) inhibitor and an autophagy inhibitor. When co-treated with 5 mM 3-MA and 10 μM RSV, cells significantly decreased the protein LC3-II/LC3-I ratio and also increased the protein expression of cleaved-caspase 3 (Figure 2c and Figure 2d). After 100 nM RAPA and 10 μM RSV pre-treatment, cells significantly increased the protein LC3-II/LC3-I ratio and also increased the protein expression of cleaved-caspase 3 (Figure 2c-d). So we think appropriately increasing autophagy could protect podocytes incubated in medium containing high glucose. While excessively increasing autophagy or overmuch decreasing autophagy might cause injure of podocytes in medium containing high glucose (Figure 2).

MicroRNA-18a-5p (a Differentially Expressed miRNA) was Significantly Downregulated in db/db Mice's Kidney and Unregulated After RSV Treated

We performed miRNA microarray analysis. The microRNA gene chip assay of the kidney of mice in the three groups (db/m group, db/db group, db/db + RSV group) showed several differentially expressed miRNAs. Differentially expressed miRNAs were identified through fold change. The threshold set for up- and downregulated genes was a fold change ≥ 2.0. Of the 3,163 known and predicted mus musculus miRNAs, 28 miRNAs were up regulated and 15 were downregulated in the db/db group compared with db/m

group. 12 miRNAs were up regulated and 21 were downregulated in the db/db + RSV group compared with db/db group. We chose 17 candidate miRNAs for further study. 13 were upregulated more than two folds in the db/db group compared with db/m group, meanwhile were downregulated more than two folds in the db/db + RSV group compared with db/db group (Table II). 4 were downregulated more than two folds in the db/db group compared with db/m group, meanwhile were upregulated more than two folds in the db/db + RSV group compared with db/db group (Table II). Among these miRNAs, miR18a-5p was downregulated in db/db mice when compared with db/m mice, while after RSV treated, miR-18a-5p was unregulated. We further validated the expression of miR-18a-5p by Real-time PCR in three independent mice of each group, which were different from the one used for array hybridization. As shown in Figure 3a, miR18a-5p expression in db/db mice was significantly downregulated than that in db/m group, and was significantly upregulated after RSV treated.

MiR-18a-5p Downregulates Apoptosis and Upregulates Autophagy by RSV

Levels of cleaved-caspase 3 protein in kidney of db/db mice were higher than db/m mice, while resveratrol significantly decreased the expressions of cleaved-caspase 3 protein in mouse kidney. Of note, there is an inverse relationship between the cleaved-caspase 3 protein expression and miR18a-5p. To further investigate the role of miR18a-5p on apoptosis and autophagy, we overexpressed and inhibited the expression of miR18a-5p in podocytes. Transfected with miR-18a-5p of inhibitors, mimics, NC, and Mock groups, RT-PCR confirmed miR-18a-5p-mimic resulted in miR-18a-5p overexpression, while miR-18a-5pinhibitor resulted in miR-18a-5p inhibition (Table III). Overexpression of miR-18a-5p resulted in significant inhibition of the expression of cleaved-caspase 3 protein, while inhibition of miR-18a-5p reversed the results (Figure 3b-c). Besides, Western blot showed that the ratio of protein LC3-II/LC3-I was decreased in cells transfected with inhibitors, whereas the ratio of LC3-

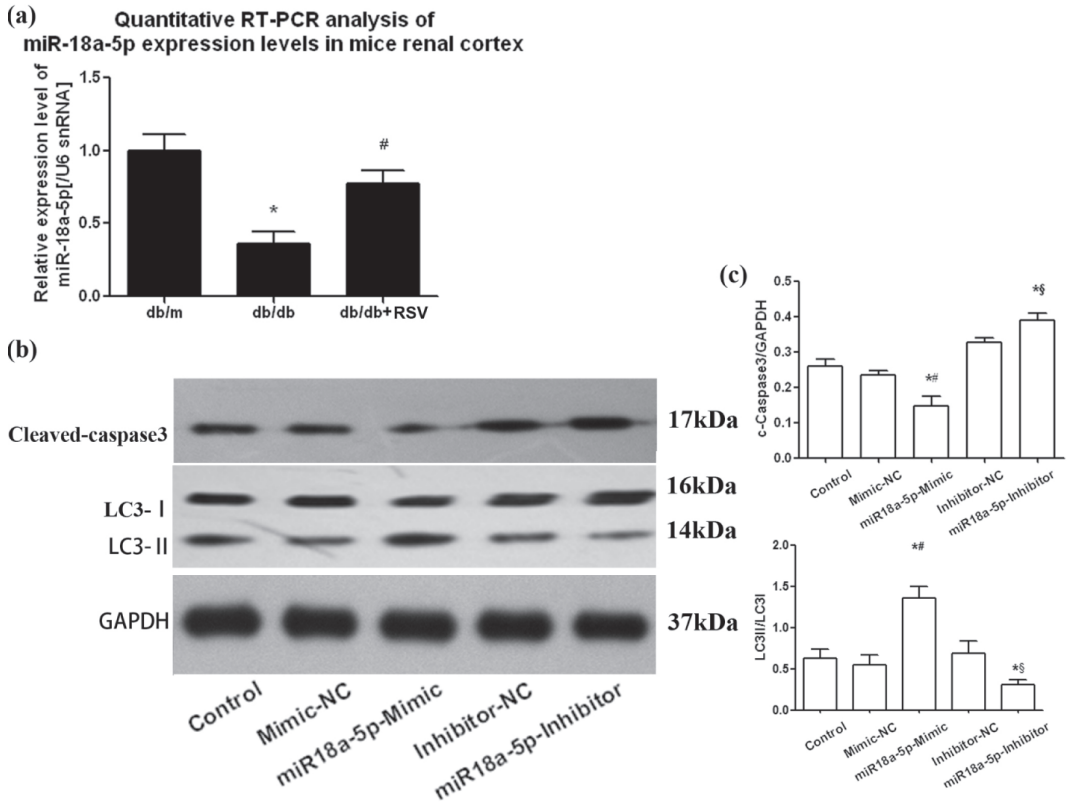

Figure 3. MiR-18a-5p inhibited apoptosis but promoted autophagy in podocytes. A: RSV significantly upregulatedmiR-18a-5p in db/db mice (*: significant difference *vs.* db/m group at $p<0.05$. #: significant difference *vs.* db/db group at $p<0.05$); B and C: Overexpression of miR-18a-5p in podocytes promoted autophagy (*: significant difference *vs.* control group at $p<0.05$. #: significant difference *vs.* Mimic NC group at $p<0.05$. §: significant difference *vs.* Inhibitor NC group at $p<0.05$).

II/LC3-I was increased in cells transfected with mimics (Figure 3b-c). So we think miR-18a-5p might be a potent negative regulator of apoptosis through strengthening autophagy.

Atactic Telangiectasis Mutation (ATM) is a Target Gene of miR-18a-5p

We used the miR Base Target database to find putative miR-18a-5p targets (www.mirbase.org), and used the PubMed database to retrieve the function of target genes. Considering that miR-18a-5p is involved in autophagy, we hypothesized that downstream miR-18a-5p target genes might be associated with autophagy. Therefore, we selected the gene (atactic telangiectasis mutation, ATM) to further study. 293T cells were transfected with the luciferase vector and miR-18a-5p overexpression vector for 48 h before the cells were lysed and tested for luciferase activity, which showed that miR-18a-5p can significantly inhibit the reported gene activity for luciferase containing ATM mRNA 3′UTR region. MiR-18a-5p mimics group had relative fluorescence activities of 0.674±0.044, which was significantly lower than 1.000 ± 0.032 in control group (p=0.002) (Figure 4a). Dual luciferase reporter gene activity test results showed that, when the 3′UTR of ATM transferred to vectors with the luciferase gene, adding miR-18a-5p, can inhibit luciferase activity. That is genetic dual luciferase report assay validated ATM was a target of miR-18a-5p.

In podocytes, transfected with miR-18a-5p of inhibitors, mimics, NC, and Mock groups, Western blot showed that the expression of ATM protein was significantly enhanced in cells transfected with inhibitors, whereas the expression of ATM protein was significantly inhibited in cells transfected with mimics (Figure 4b-c).

The mRNA ATM was expected to involve in the effect of resveratrol on mice, thus expression levels of proteins ATM/GAPDH were determined by Western blots analysis. The levels of ATM protein in kidney of db/db mice, were higher than that in db/m mice, while resveratrol significantly decreased ATM levels (Figure 5a-b). So we think resveratrol could inhibit ATM expression in db/db mice.

Knockdown of ATM by siRNA increase autophagy and reduce apoptosis

Since miR18a-5p mimic could increase autophagy and decrease apoptosis, and ATM has been considered to be a target gene of miR18a-5p, which inhibits ATM, we guess ATM may be in-

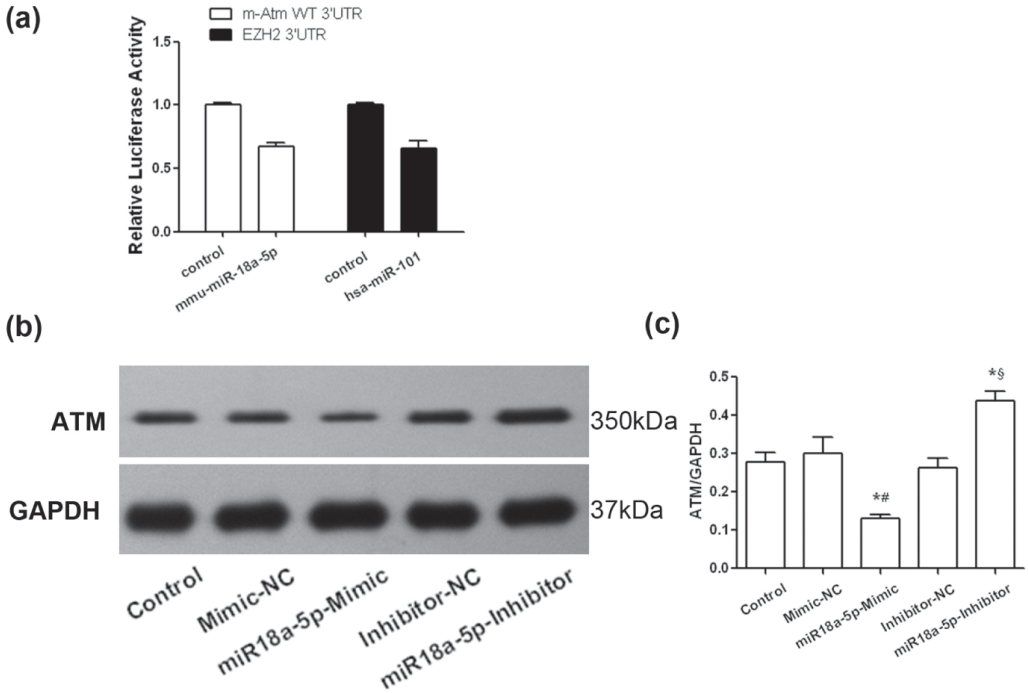

Figure 4. ATM is the target of miRNA-18a-5p. ***A,*** ATM in 293T cells was downregulated after transfection with miR-18a-5p mimics; ***B*** and ***C,*** ATM was inhibited in podocytes transfected with miRNA-18a-5p mimics.

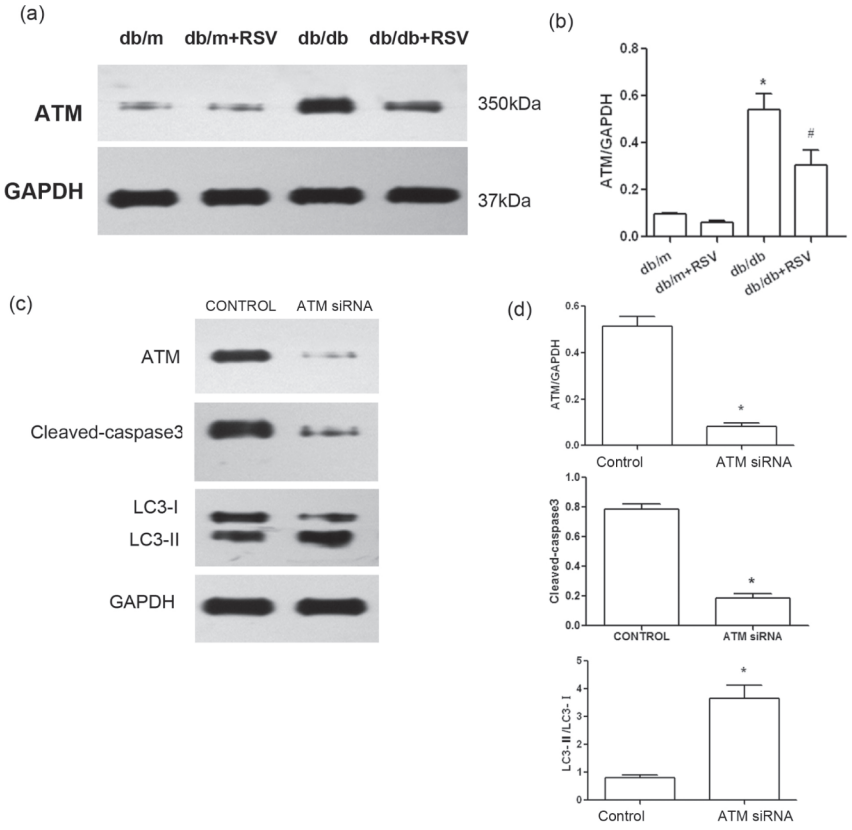

Figure 5. Knockdown of ATM induced autophagy. ***A*** and ***B*,** RSV decreased ATM levels in db/db mice's renal cortex; ***C*** and ***D*,** knockdown of ATM by siRNA inhibited apoptosis but promoted autophagy in podocytes (*: significant difference *vs.* Control at $p<0.05$).

volved in autophagy and apoptosis. We next investigated whether suppression of ATM by siRNA could promote autophagy and inhibit apoptosis. The results showed that the downregulation of cleaved caspase 3 and the enhanced ratio of protein LC3-II/LC3-I were seen in cells transfected with ATM siRNA, whereas treatment with control siRNA had no effect (Figure 5c-d). Taken together, these findings suggest that the effect of miR-18a-5p in autophagy activity and apoptosis might be *via* targeting ATM (Figure 5).

Discussion

Clinical features of diabetic nephropathy include elevated urinary albumin excretion. The key change in diabetic glomerulopathy is loss of podocytes. Podocytes have a very limited capacity for cell division and replacement[23]. Autophagy plays a critical role in removing protein aggregates and damaged organelles, promoting cell survival and tissue homeostasis[24]. Deficiency in autophagy enhances susceptibility to development of glomerular diseases, and autophagy represents a stress adaptive response of podocytes that is cytoprotective against glomerular disease. Evidence suggested that dysregulated autophagy is implicated in the pathogenesis of diabetic nephropathy. Thus, targeting the autophagic pathway to activate and restore autophagy activity might be renoprotective[2,3,6,25-27]. Impaired autophagy evidenced by renal accumulation of p62/Sequestosome 1 (SQSTM1), substrate of autophagy-lysosomal degradation pathway, was also shown in STZ-induced diabetic mice[28] and Wistar fatty rats[29]. Evidence of impaired autophagy has also been observed in kidney biopsy samples from patients with type 2 diabetes, exhibiting accumulation of p62/SQSTM1 protein in proximal tubular cells, suggesting that deficiency in autophagy also occurs in human type 2 diabetes[30].

Sharma et al[31] reported that treatment with resveratrol (5 mg or 10 mg/kg orally) for 2 weeks

improved urinary protein excretion and renal oxidative stress in streptozotocin- (STZ-) induced diabetic rats.

Kitada et al[12] also reported that resveratrol treatment (400 mg/kg, orally, administered at concentration of 0.3% resveratrol) alleviated albuminuria and histological mesangial expansion and reduced the increased levels of renal oxidative stress and inflammation in the kidneys of db/db mice through the scavenging of ROS and normalizing manganese (Mn)-SOD function by decreasing its levels of nitrosative modification. Kitada and Koya[32] summarized the protective effects of resveratrol against several types of renal injury and discussed the mechanisms involved. There are two proposed mechanisms by which resveratrol exerts cytoprotection: (1) resveratrol attenuates oxidative stress; (2) resveratrol activates SIRT1, which is an NAD^+-dependent deacetylase, directly or indirectly *via* AMPK activation. SIRT1 plays an important role in the regulation of oxidative stress, inflammation, apoptosis, stress resistance, mitochondrial biogenesis, autophagy, and glucose-lipid metabolism, *via* the deacetylation of many substrates.

Our study showed that treatment with resveratrol (100 mg/kg/day orally) for 12 weeks attenuated the albuminuria. We found that the levels of protein LC3-II/LC3-I in kidney of db/db mice were lower than that in db/m mice, reflecting the level of autophagy is insufficient relatively in db/db mice. We also found that resveratrol could significantly increase synaptopodin expression and enhance the levels of LC3-II protein in the renal cortex of diabetic mice. We demonstrated that resveratrol protected podocytes, by decreasing the levels of apoptosis and slightly increasing the levels of autophagy in the renal cortex of db/db mice.

In our previous report, we showed that podocytes under continuous high glucose conditions *in vitro* were found to exhibit a low constitutive level of LC3-II/LC3-I, a robust marker of autophagosomes, suggesting a high basal level of autophagic activity. High basal level of autophagy in podocytes became defective and could facilitate the podocyte injury. We found there was a complex relationship between autophagy promotion and apoptosis inhibition. RSV protects podocytes from high glucose-induced apoptosis. Further *in vitro* studies also showed that resveratrol enhanced protein expression of LC3-II and inhibited cleaved-caspase 3 protein in the cultured podocytes incubated in medium containing high glucose. Using the popular inhibitor of the autophagic pathway 3-MA, we found that inhibition of autophagy could induce podocyte apoptosis. Using an activator of autophagy, RAPA, we found that strongly increasing autophagy could also induce podocyte apoptosis. We think that properly high levels of constituent autophagy in non-renewable cells (such as podocytes) might be important to preserve cell viability. Then, we found that high glucose levels enhance apoptosis, which was inhibited by resveratrol through enhanced autophagy in cultured podocytes. We think RSV, an autophagy promoter, ameliorates diabetic nephropathy *via* increasing autophagy. However, excessive autophagy can also contribute to cell death and worsening proteinuria. Future investigations are necessary to uncover the precise functional roles of autophagy in glomerular and tubular injury related to DN that will further advance our understanding of the role of autophagy in the kidney and guide potential therapies.

MiRNAs are linked to regulation of autophagy pathway[21]. Matboli et al[33] found that, in diabetic rats, caffeic acid intake resulted in autophagy genes upregulation [RB 1-inducible coiled coil protein (RB1CC1), microtubule-associated proteins 1A/1B light chain 3 (MAP1LC3B), and autophagy related gene (ATG-12)] with simultaneous reduction in their epigenetic regulators; miRNA-133b, -342 and 30a, respectively.

In our studies, we found that several microRNAs changed after RVS treated in the renal cortex of the db/db mice, such as miR-133a-3p, miR-188-5p, miR-206-3p, miR-18a-5p, miR-382-5p, miR-541-5p and miR-714. Next, we found miR-18a-5p mimic increased autophagy and decreased apoptosis, while miR-18a-5p inhibitor acted the opposite in podocytes cultured in high glucose. So, we guessed that kidney protection by RVS was through the upregulation of miRNA-18a-5p.

ATM protein kinase, which is a master regulator of the DNA damage response, coordinates checkpoint activation, DNA repair, and metabolic changes in eukaryotic cells in response to DNA double-strand breaks and oxidative stress. Loss of ATM activity in humans results in the pleiotropic neurodegeneration disorder ataxia-telangiectasia[34]. The responses of ATM to resveratrol treatment in normal and transformed cells may display differently. For example, resveratrol can lead to an autophosphorylation of ATM on Ser1981 and a phosphorylation of p53 on Ser15 in transformed cells (HEK293T and HCT116) involving reactive oxygen species (ROS), but this is largely unchan-

ged in normal human fibroblasts (GM08399)[35]. The resveratrol-induced ATM signaling effect was inhibited by the disulfide-specific reducing agent Tris (2-carboxyethyl) phosphine and the antioxidant N-acetyl cysteine, suggesting that high oxidative stress was involved in ATM signaling of resveratrol in transformed cells to block cancer cell proliferation[35].

In our study, we confirmed ATM was the target gene of miR-18a-5p, evidenced by decreased activity of luciferase reporter vector of ATM after miR-18a-5p treatment. *In vivo*, after RVS treated, the levels of ATM were decreased in the renal cortex of db/db mice. Silencing ATM gene upregulated the ratio of LC3-II/LC3-I and decreased cleaved-caspase-3 expression in cultured podocytes, indicating that miR-18a-5p mediated the autophagy activity and apoptosis via inhibiting ATM.

Conclusions

We showed that miRNA-18a-5p is activated by RSV and points to a critical role for miRNA-18a-5p in the control of autophagy activity through ATM. These findings suggested that miRNA-18a-5p may represent a promising therapeutic target for preventing and attenuating diabetic nephropathy.

Acknowledgments

We thank the entire staff at the Biotech Treatment Center, The Second Affiliated Hospital of Nanjing Medical University, Nanjing, China for their excellent technical assistance with this research. This work was supported by grants from the National Natural Science Foundation of China (Grant nos 81270896, 81100577) and Six Talent Peaks Project in Jiangsu Province (Grant nos 2013-WSN-049, 2015-WSN-016).

Conflict of interest

The authors declare no conflicts of interest.

References

1) Levine B, Ranganathan R. Autophagy: snapshot of the network. Nature 2010; 466: 38-40.
2) Wang Z, Choi ME. Autophagy in kidney health and disease. Antioxid Redox Signal 2014; 20: 519-537.
3) Fang L, Zhou Y, Cao H, Wen P, Jiang L, He W, Dai C, Yang J. Autophagy attenuates diabetic glomerular damage through protection of hyperglycemia-induced podocyte injury. PLoS One 2013; 8: e60546.
4) Fang L, Li X, Luo Y, He W, Dai C, Yang J. Autophagy inhibition induces podocyte apoptosis by activating the pro-apoptotic pathway of endoplasmic reticulum stress. Exp Cell Res 2014; 322: 290-301.
5) Hartleben B, Godel M, Meyer-Schwesinger C, Liu S, Ulrich T, Kobler S, Wiech T, Grahammer F, Arnold SJ, Lindenmeyer MT, Cohen CD, Pavenstadt H, Kerjaschki D, Mizushima N, Shaw AS, Walz G, Huber TB. Autophagy influences glomerular disease susceptibility and maintains podocyte homeostasis in aging mice. J Clin Invest 2010; 120: 1084-1096.
6) Ding Y, Choi ME. Autophagy in diabetic nephropathy. J Endocrinol 2015; 224: R15-R30.
7) Wolf G, Chen S, Ziyadeh FN. From the periphery of the glomerular capillary wall toward the center of disease: podocyte injury comes of age in diabetic nephropathy. Diabetes 2005; 54: 1626-1634.
8) Quaggin SE. Transcriptional regulation of podocyte specification and differentiation. Microsc Res Tech 2002; 57: 208-211.
9) Tharaux PL, Huber TB. How many ways can a podocyte die? Semin Nephrol 2012; 32: 394-404.
10) Xiong J, Xia M, Xu M, Zhang Y, Abais JM, Li G, Riebling CR, Ritter JK, Boini KM, Li PL. Autophagy maturation associated with CD38-mediated regulation of lysosome function in mouse glomerular podocytes. J Cell Mol Med 2013; 17: 1598-1607.
11) Kim MY, Lim JH, Youn HH, Hong YA, Yang KS, Park HS, Chung S, Ko SH, Shin SJ, Choi BS, Kim HW, Kim YS, Lee JH, Chang YS, Park CW. Resveratrol prevents renal lipotoxicity and inhibits mesangial cell glucotoxicity in a manner dependent on the AMPK-SIRT1-PGC1alpha axis in db/db mice. Diabetologia 2013; 56: 204-217.
12) Kitada M, Kume S, Imaizumi N, Koya D. Resveratrol improves oxidative stress and protects against diabetic nephropathy through normalization of Mn-SOD dysfunction in AMPK/SIRT1-independent pathway. Diabetes 2011; 60: 634-643.
13) Lei LT, Chen JB, Zhao YL, Yang SP, He L. Resveratrol attenuates senescence of adipose-derived mesenchymal stem cells and restores their paracrine effects on promoting insulin secretion of INS-1 cells through Pim-1. Eur Rev Med Pharmacol Sci 2016; 20: 1203-1213.
14) Morselli E, Maiuri MC, Markaki M, Megalou E, Pasparaki A, Palikaras K, Criollo A, Galluzzi L, Malik SA, Vitale I, Michaud M, Madeo F, Tavernarakis N, Kroemer G. Caloric restriction and resveratrol promote longevity through the Sirtuin-1-dependent induction of autophagy. Cell Death Dis 2010; 1: e10.
15) Howitz KT, Bitterman KJ, Cohen HY, Lamming DW, Lavu S, Wood JG, Zipkin RE, Chung P, Kisielewski A, Zhang LL, Scherer B, Sinclair DA. Small molecule activators of sirtuins extend Saccharomyces cerevisiae lifespan. Nature 2003; 425: 191-196.

16) Chen ML, Yi L, Jin X, Liang XY, Zhou Y, Zhang T, Xie Q, Zhou X, Chang H, Fu YJ, Zhu JD, Zhang QY, Mi MT. Resveratrol attenuates vascular endothelial inflammation by inducing autophagy through the cAMP signaling pathway. Autophagy 2013; 9: 2033-2045.

17) Kim ES, Chang H, Choi H, Shin JH, Park SJ, Jo YK, Choi ES, Baek SY, Kim BG, Chang JW, Kim JC, Cho DH. Autophagy induced by resveratrol suppresses alpha-MSH-induced melanogenesis. Exp Dermatol 2014; 23: 204-206.

18) Zhang J, Song X, Cao W, Lu J, Wang X, Wang G, Wang Z, Chen X. Autophagy and mitochondrial dysfunction in adjuvant-arthritis rats treatment with resveratrol. Sci Rep 2016; 6: 32928.

19) Duan WJ, Liu FL, He RR, Yuan WL, Li YF, Tsoi B, Su WW, Yao XS, Kurihara H. Autophagy is involved in the effects of resveratrol on prevention of splenocyte apoptosis caused by oxidative stress in restrained mice. Mol Nutr Food Res 2013; 57: 1145-1157.

20) Hammond SM. An overview of microRNAs. Adv Drug Deliv Rev 2015; 87: 3-14.

21) Su Z, Yang Z, Xu Y, Chen Y, Yu Q. MicroRNAs in apoptosis, autophagy and necroptosis. Oncotarget 2015; 6: 8474-8490.

22) Mundel P, Reiser J, Zuniga MBA, Pavenstadt H, Davidson GR, Kriz W, Zeller R. Rearrangements of the cytoskeleton and cell contacts induce process formation during differentiation of conditionally immortalized mouse podocyte cell lines. Exp Cell Res 1997; 236: 248-258.

23) Kobayashi N. Mechanism of the process formation; podocytes vs. neurons. Microsc Res Tech 2002; 57: 217-223.

24) Klionsky DJ, Emr SD. Autophagy as a regulated pathway of cellular degradation. Science 2000; 290: 1717-1721.

25) Takabatake Y, Kimura T, Takahashi A, Isaka Y. Autophagy and the kidney: health and disease. Nephrol Dial Transplant 2014; 29: 1639-1647.

26) Hartleben B, Godel M, Meyer-Schwesinger C, Liu S, Ulrich T, Kobler S, Wiech T, Grahammer F, Arnold SJ, Lindenmeyer MT, Cohen CD, Pavenstadt H, Kerjaschki D, Mizushima N, Shaw AS, Walz G, Huber TB. Autophagy influences glomerular disease susceptibility and maintains podocyte homeostasis in aging mice. J Clin Invest 2010; 120: 1084-1096.

27) Kume S, Yamahara K, Yasuda M, Maegawa H, Koya D. Autophagy: emerging therapeutic target for diabetic nephropathy. Semin Nephrol 2014; 34: 9-16.

28) Vallon V, Rose M, Gerasimova M, Satriano J, Platt KA, Koepsell H, Cunard R, Sharma K, Thomson SC, Rieg T. Knockout of Na-glucose transporter SGLT2 attenuates hyperglycemia and glomerular hyperfiltration but not kidney growth or injury in diabetes mellitus. Am J Physiol Renal Physiol 2013; 304: F156-F167.

29) Kitada M, Takeda A, Nagai T, Ito H, Kanasaki K, Koya D. Dietary restriction ameliorates diabetic nephropathy through anti-inflammatory effects and regulation of the autophagy via restoration of Sirt1 in diabetic Wistar fatty (fa/fa) rats: a model of type 2 diabetes. Exp Diabetes Res 2011; 2011: 908185.

30) Yamahara K, Kume S, Koya D, Tanaka Y, Morita Y, Chin-Kanasaki M, Araki H, Isshiki K, Araki S, Haneda M, Matsusaka T, Kashiwagi A, Maegawa H, Uzu T. Obesity-mediated autophagy insufficiency exacerbates proteinuria-induced tubulointerstitial lesions. J Am Soc Nephrol 2013; 24: 1769-1781.

31) Sharma S, Anjaneyulu M, Kulkarni SK, Chopra K. Resveratrol, a polyphenolic phytoalexin, attenuates diabetic nephropathy in rats. Pharmacology 2006; 76: 69-75.

32) Kitada M, Koya D. Renal protective effects of resveratrol. Oxid Med Cell Longev 2013; 2013: 568093.

33) Matboli M, Eissa S, Ibrahim D, Hegazy M, Imam SS, Habib EK. Caffeic acid attenuates diabetic kidney disease via modulation of autophagy in a high-fat diet/streptozotocin- induced diabetic rat. Sci Rep 2017; 7: 2263.

34) Farooqi AA, Attar R, Arslan BA, Romero MA, Ul HM, Qadir MI. Recently emerging signaling landscape of ataxia-telangiectasia mutated (ATM) kinase. Asian Pac J Cancer Prev 2014; 15: 6485-6488.

35) Lee JH, Guo Z, Myler LR, Zheng S, Paull TT. Direct activation of ATM by resveratrol under oxidizing conditions. PLoS One 2014; 9: e97969.